On Transverse Emittance Fluctuations as measured by Tevatron Flying Wire Horizontal Detector at E11 location at 150GeV Version 3.0

August 28th 2003

Krzysztof Genser
Computing Division, Fermilab

Abstract

We study the origin of the Transverse Emittance Fluctuations as measured by Tevatron Flying Wire Horizontal Detector at E11 location. We conclude, that the fluctuations are correlated with the direction of the wire flight.

1 Introduction

We study Tevatron Transverse Emittance measurements done using Flying Wire (FW) (See ref [2]) Detector. The Flying Wires were used to measure the transverse beam spread. The Sampled Bunch Display (SBD) system was used to measure longitudinal beam spread.

2 Data Selection

The stores for this analysis were selected from Spring 2003 running period when The FW freshness number (ACcelerator NETwork (ACNET) variable T:FWFRSH) was not reset so that one could assume a one to one correlation between the freshness number parity and the direction of flight of the detector wire. The requirement resulted in store range 2426-2546. The Tevatron Case chosen for analysis was "Inject Protons" (with the beam energy of 150GeV) as this is one of the cases where the same bunches are measured for each parity of the freshness number. The other requirements imposed on the data were:

1. The FW freshness number in Case "Initiate Collisions" had to non zero and be incremented by at least one with respect to a previous Case Set (except for Set 1 where it was required to be greater than 0 only);
2. The Transverse Emittance as measured by the FW E11 Detector (combined with SBD data in the horizontal cases) had to be between 0 and 50 ($\pi \cdot mm \cdot mrad$) (to avoid both nonphysical or difficult to measure cases);
3. the bunch width sigma had to correspond to the emittance reported by the Front End system within 10% to reject cases with data aquisition problems;
4. bunch number had to be smaller than 35 to reject bunches measured only once;

3 Emittance calculations

The following formulas were used to calculate the Horizontal and Vertical (Normalized) Emittances:

$$\varepsilon_h = 6\left(\sigma^2 - (\frac{\delta p}{p})^2 D^2\right)\frac{\gamma_L}{\beta} \qquad \varepsilon_v = 6\sigma^2\frac{\gamma_L}{\beta}$$

where

$$\delta p = \delta t * (83.293 + \delta t * (-10.562 + \delta t * 0.8023)) \text{ (See ref [1])}$$

δt is the T:SBD[A,P]SS ACNET variable (longitudinal beam bunch spread in ns), p is the beam momentum in GeV, γ_L is the Lorentz gamma, σ are bunch width as measured by each of the detectors (ACNET variables T:SL[A,P]S[H,V], T:FW[H,V,E][A,P]SG). In the FW case the width is the arithmetic average of the two measurements (for both of the wire passes trough the beam). The dispersion (D) and β lattice functions used for E11, E17, C11 (location of the SL detector) are shown in Table 1.

Detector	beta Function [m]	dispersion Function [m]
FW E11H p & $\overline{p}$	80.161	2.030
FW E11V p & $\overline{p}$	80.804	
FW E17H p & $\overline{p}$	68.157	5.278
SL C11H p	50.005	1.517
SL C11H $\overline{p}$	34.040	1.182
SL C11V p	107.862	
SL C11V $\overline{p}$	101.648	

Table 1: Tevatron beta and dispersion functions for corresponding measurement locations

4 Emittance Measurement Dependence on Direction of Wire Flight

The plots on Fig 1 show sigma and centroid for Horizontal Flying Wire Detector at the E11 location. One can clearly see that the value of both sigma and centroid depend on the direction of the flight of the wire. The size of the effect is about $50\mu m$. The resulting effect on the emittance is about 10% (Fig 6).

The other two detectors do not exhibit such big measurement discrepancies (see Fig 7–18). There is a hint of a flight direction dependence in the E17 detector emittance plot (Fig 12) but the size of the effect is only about 3% for given emittances.

The plots of the remainder of the bunch number (0-35) divided by two versus the remainder of Flying Wire Data Freshens variable divided by two shown in Fig 6, 12, 18 show that for the given collection of stores there was no correlation between bunch number parity and the direction of flight.

5 Flying Wire Pass One and Pass Two Data Dependence on Direction of Wire Flight

The plots on Fig 2 and 3 show pass one and pass two sigma and centroid for Horizontal Flying Wire Detector at the E11 location. In the case of this detector pass one and pass two distribution are similar to the average distributions from Fig 1. Corresponding distributions for E17 Horizontal Flying Wire Detector and E11 Vertical Detector are shown on Fig 8,9 and Fig 14,3. It looks like in the case of the E11 Vertical Detector the pass one distributions for different freshness parity are shifted in the opposite way compared to pass two distributions whereas E17 Horizontal Detector distributions seem to be slightly shifted in the pass one case.

Plots on Fig 4 show differences between pass two and pass one sigmas and centroids for Horizontal Detector at E11. They do not seem to depend on the direction of the flight of the wire. Plots on Fig 4 show difference between pass two and pass one sigmas versus difference between pass two and pass one centroids for all flight directions and for each direction separately. There seems to be no correlation between the variables on the later plots.

Similar plots for E17 Horizontal and E11 Vertical Detectors are shown of Fig 10–11 and Fig 16–17. Here, in both cases the sigma difference depends on the wire flight direction. E11 Vertical detector is the only detector where the centroid pass two pass one difference distribution depends on the wire flight direction and exhibits an non bell like peak structure.

6 Conclusions

Given the above, we conclude, that the emittance fluctuations as measured by the E11 Flying Wire Detector are due to a detector effect and are correlated with the direction of the wire flight.

Acknowledgments

We would like to thank Stephen Pordes and Jean Slaughter for their suggestions and comments.

References

[1] M. Church, *A Study of the Emittances of P1 during Proton Injections for Store 2070*, talk on 01/16/2003, http://www-bd.fnal.gov/sdahomepage/osda/devices/p1_2070_study_pdf.pdf

[2] S. Pordes et al, *Measurements of Proton and Antiproton beam intensities in the Tevatron*, Particle Accelerator Conference, Portland, Oregon, USA, May 12-16, 2003

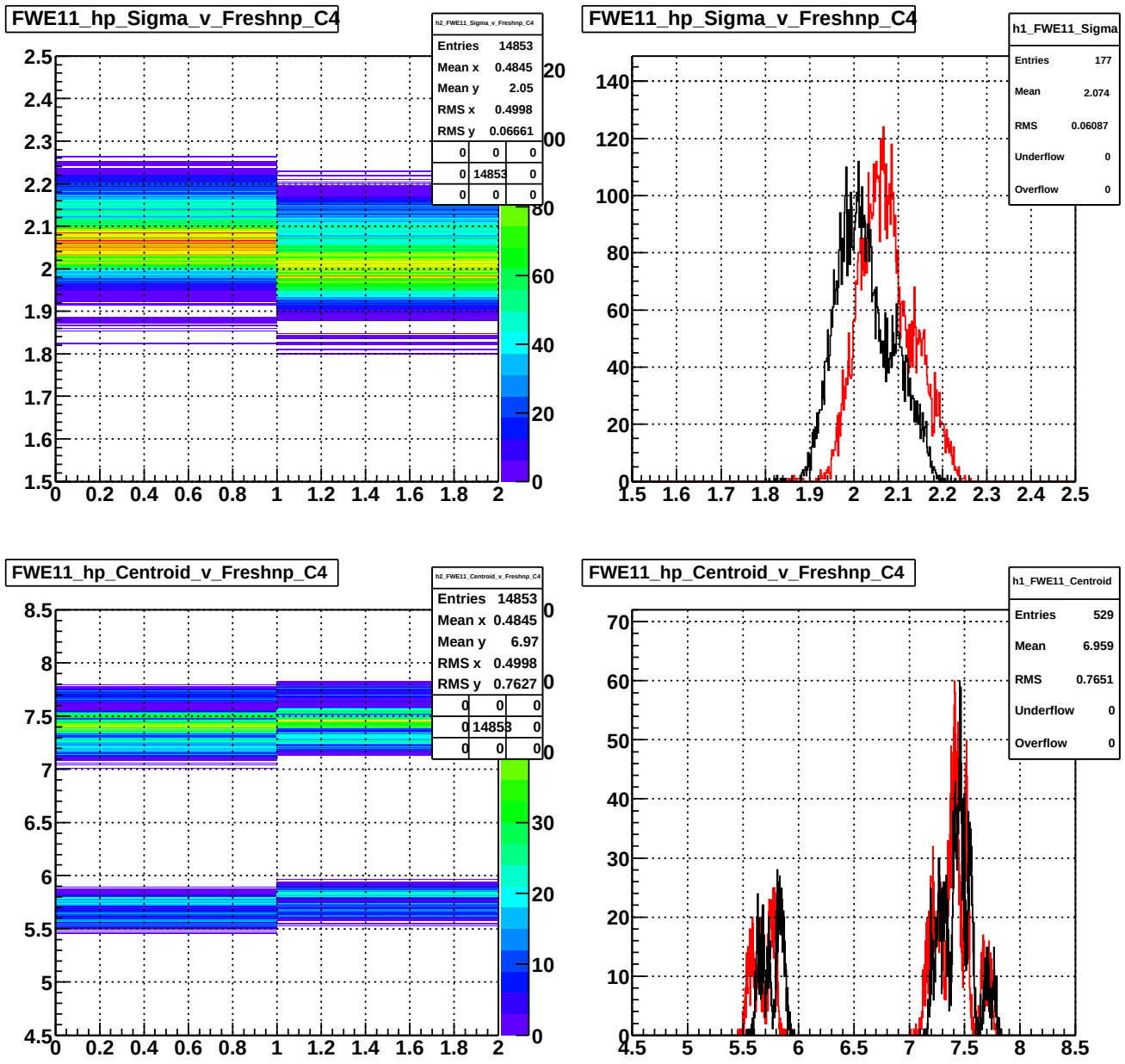

Figure 1: Proton beam, horizontal detector: Performance of the Flying Wire Detector at the E11 location during Tevatron Inject Proton case: sigma of the bunch width distribution (in *mm*) of the FW detector (based on the T:FW[E,H,V][A,P]SE ACNET variable) versus the remainder of Flying Wire Data Freshness variable divided by two (based on the T:FWFRSH ACNET variable); sigma of the bunch width distribution (in *mm*) for odd values of Data Freshness in black and for even values of Data Freshness in red; bunch centroid (in *mm*) position (based on the T:FW[E,H,V][A,P]CE ACNET variable) versus versus the remainder of Flying Wire Data Freshness variable divided by two; bunch centroid (in *mm*) position for odd values of Data Freshness in black and for even values of Data Freshness in red.

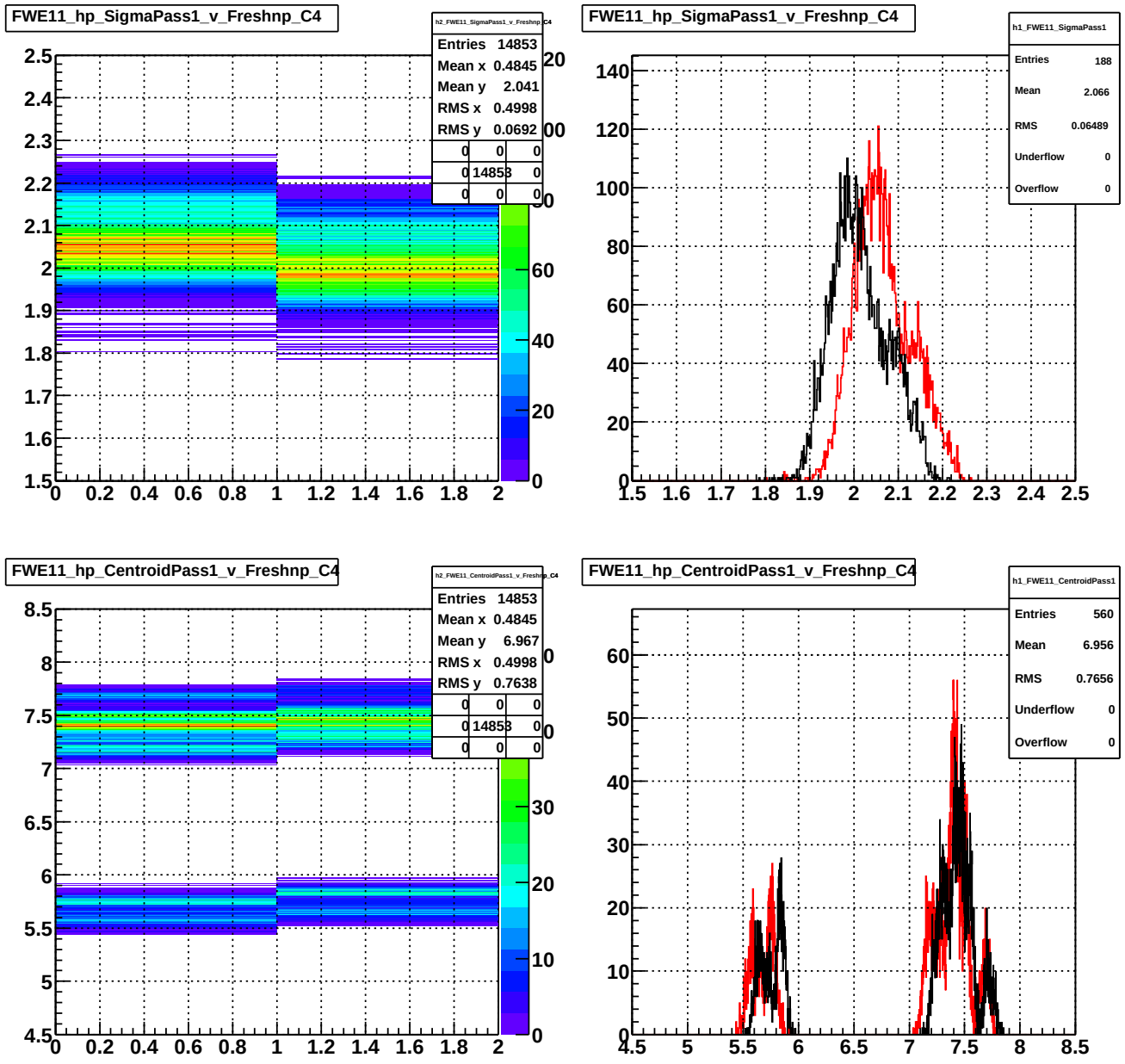

Figure 2: Proton beam, horizontal detector: Performance of the Flying Wire Detector at the E11 location during Tevatron Inject Proton case: pass one sigma of the bunch width distribution (in *mm*) of the FW detector (based on the T:FW[E,H,V][A,P]SE ACNET variable) versus the remainder of Flying Wire Data Freshness variable divided by two (based on the T:FWFRSH ACNET variable); pass one sigma of the bunch width distribution (in *mm*) for odd values of Data Freshness in black and for even values of Data Freshness in red; bunch pass one centroid (in *mm*) position (based on the T:FW[E,H,V][A,P]CE ACNET variable) versus versus the remainder of Flying Wire Data Freshness variable divided by two; bunch pass one centroid (in *mm*) position for odd values of Data Freshness in black and for even values of Data Freshness in red.

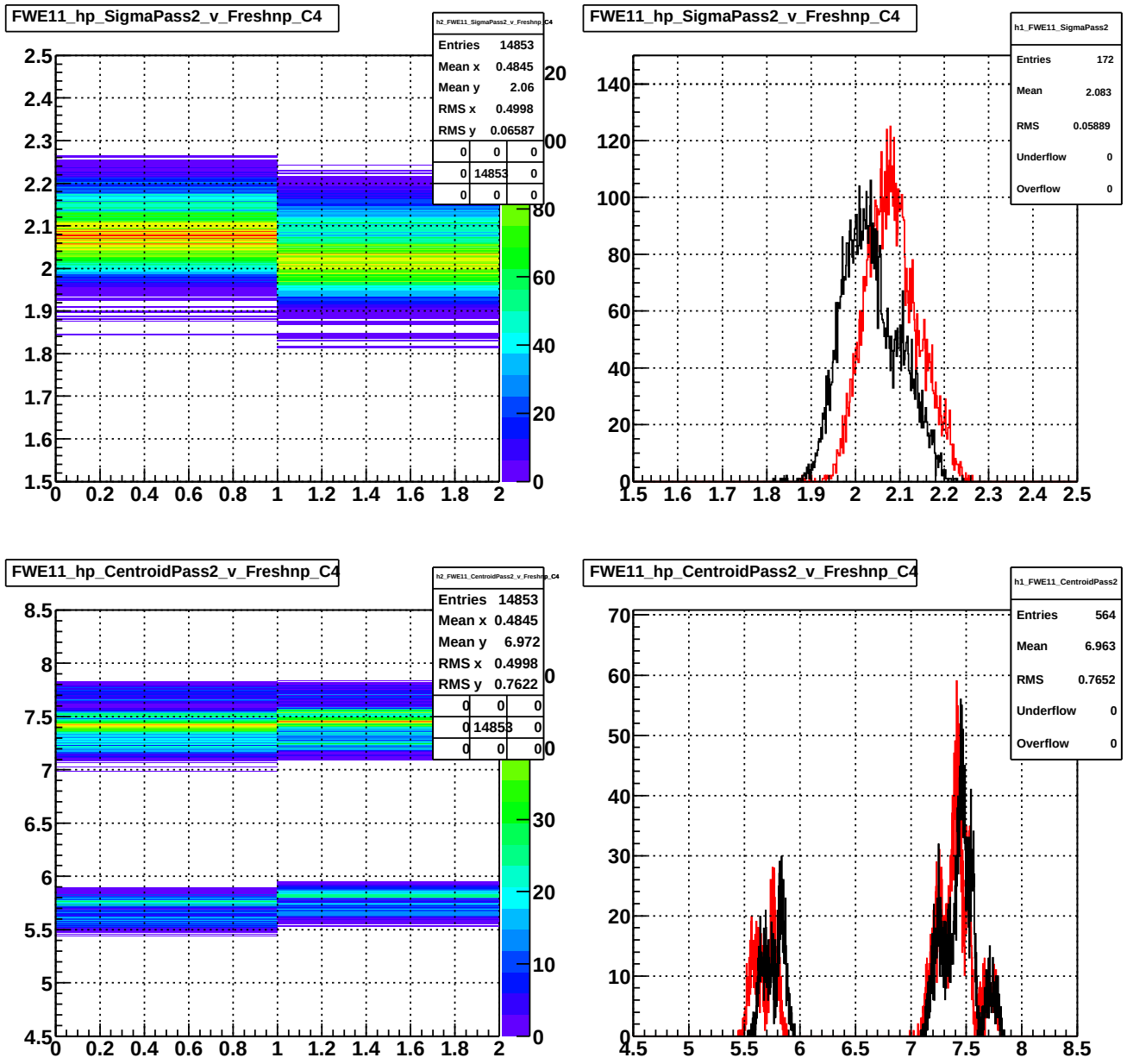

Figure 3: Proton beam, horizontal detector: Performance of the Flying Wire Detector at the E11 location during Tevatron Inject Proton case: pass two sigma of the bunch width distribution (in *mm*) of the FW detector (based on the T:FW[E,H,V][A,P]SE ACNET variable) versus the remainder of Flying Wire Data Freshness variable divided by two (based on the T:FWFRSH ACNET variable); pass two sigma of the bunch width distribution (in *mm*) for odd values of Data Freshness in black and for even values of Data Freshness in red; bunch pass two centroid (in *mm*) position (based on the T:FW[E,H,V][A,P]CE ACNET variable) versus versus the remainder of Flying Wire Data Freshness variable divided by two; bunch pass two centroid (in *mm*) position for odd values of Data Freshness in black and for even values of Data Freshness in red.

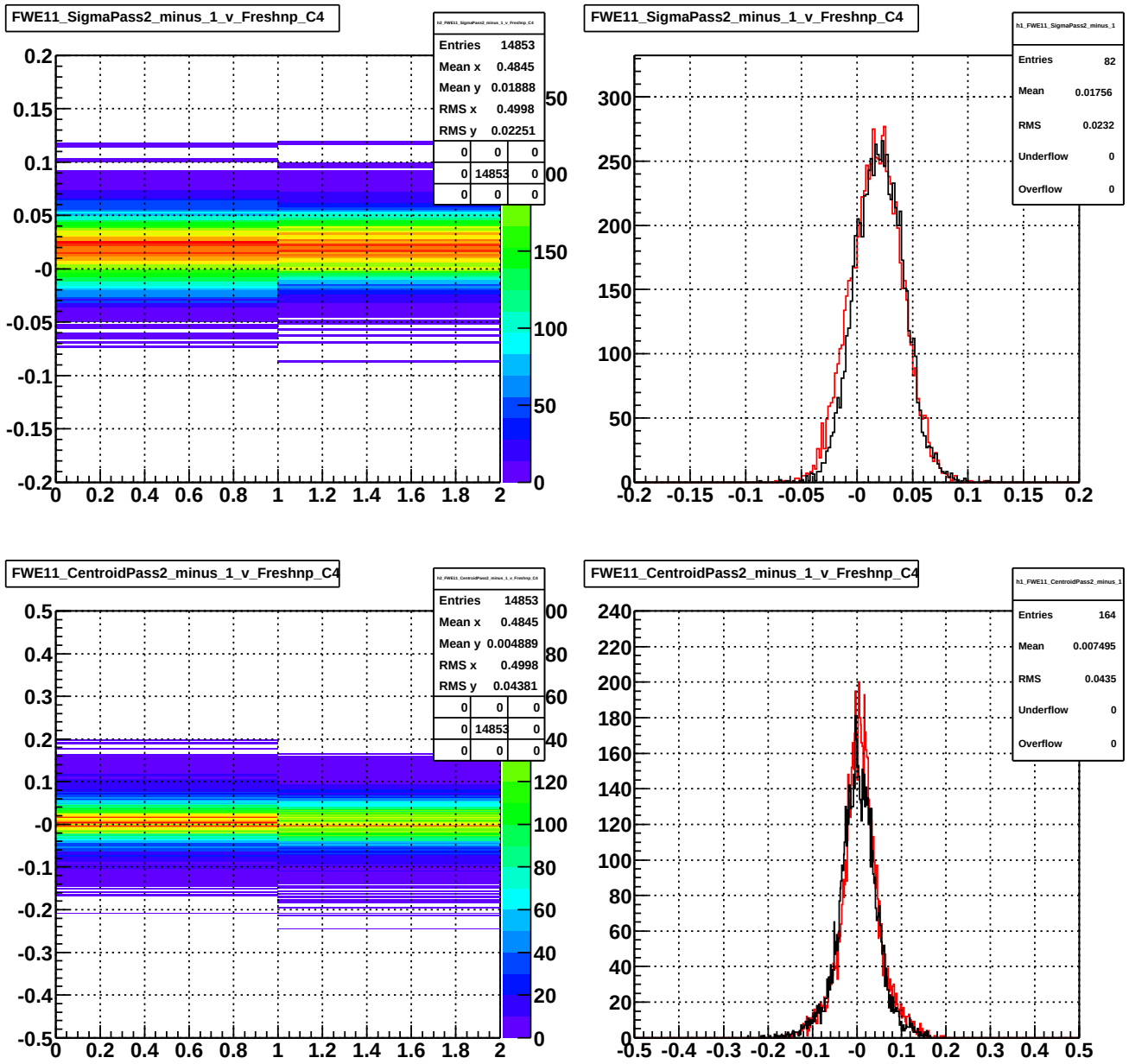

Figure 4: Proton beam, horizontal detector: Performance of the Flying Wire Detector at the E11 location during Tevatron Inject Proton case: sigma pass one minus pass two of the bunch width distribution (in *mm*) of the FW detector (based on the T:FW[E,H,V][A,P]SE ACNET variable) versus the remainder of Flying Wire Data Freshness variable divided by two (based on the T:FWFRSH ACNET variable); sigma pass one minus pass two of the bunch width distribution (in *mm*) for odd values of Data Freshness in black and for even values of Data Freshness in red; bunch centroid pass one minus pass two (in *mm*) position (based on the T:FW[E,H,V][A,P]CE ACNET variable) versus versus the remainder of Flying Wire Data Freshness variable divided by two; bunch centroid pass one minus pass two (in *mm*) position for odd values of Data Freshness in black and for even values of Data Freshness in red.

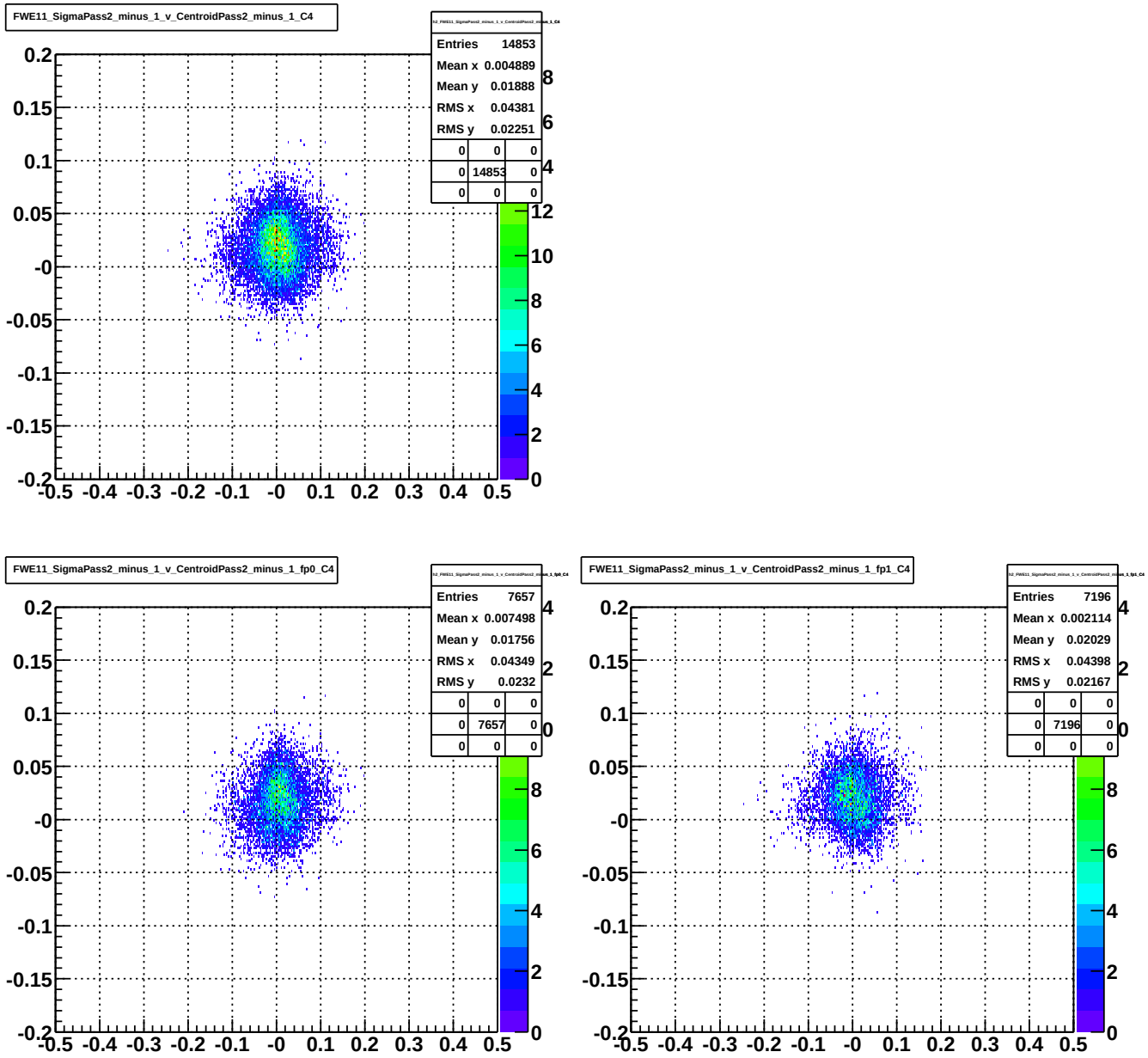

Figure 5: Proton beam, horizontal detector: Performance of the Flying Wire Detector at the E11 location during Tevatron Inject Proton case: sigma pass one minus pass two of the bunch width distribution (in *mm*) of the FW detector (based on the T:FW[E,H,V][A,P]SE ACNET variable) versus bunch centroid pass one minus pass two (in *mm*) position (based on the T:FW[E,H,V][A,P]CE ACNET variable); sigma pass one minus pass two of the bunch width distribution (in *mm*) of the FW detector (based on the T:FW[E,H,V][A,P]SE ACNET variable) versus bunch centroid pass one minus pass two (in *mm*) position (based on the T:FW[E,H,V][A,P]CE ACNET variable) for even values of Flying Wire Data Freshness (based on the T:FWFRSH ACNET variable); sigma pass one minus pass two of the bunch width distribution (in *mm*) of the FW detector (based on the T:FW[E,H,V][A,P]SE ACNET variable) versus bunch centroid pass one minus pass two (in *mm*) position (based on the T:FW[E,H,V][A,P]CE ACNET variable) for odd values of Flying Wire Data Freshness (based on the T:FWFRSH ACNET variable).

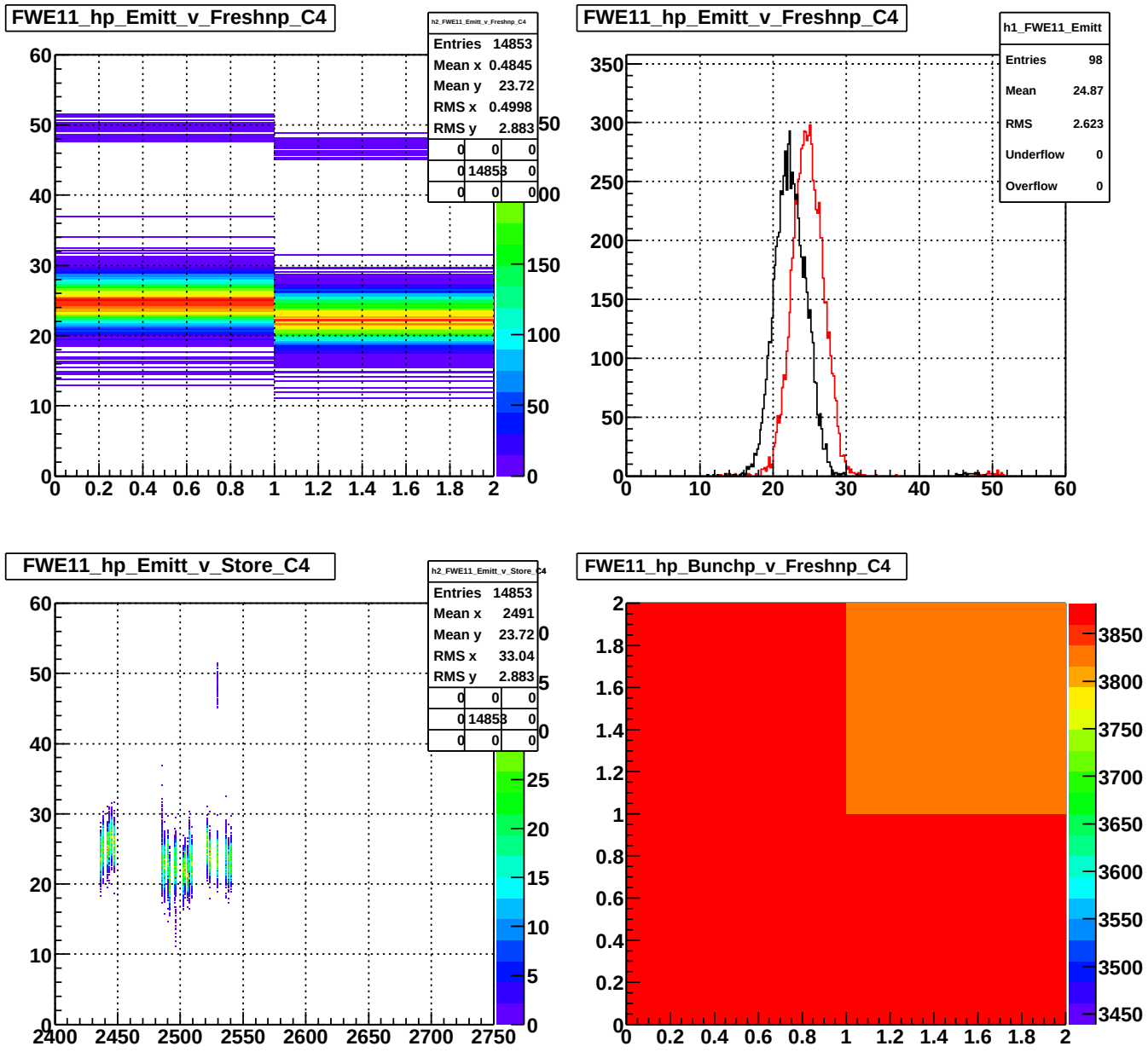

Figure 6: Proton beam, horizontal detector: Performance of the Flying Wire Detector at the E11 location during Tevatron Inject Proton case: bunch emittance (in $\pi \cdot mm \cdot mrad$) versus the remainder of Flying Wire Data Freshness variable divided by two (based on the T:FWFRSH ACNET variable); bunch emittance (in $\pi \cdot mm \cdot mrad$) for odd values of Data Freshness in black and for even values of Data Freshness in red; bunch emittance (in $\pi \cdot mm \cdot mrad$) versus store number; the remainder of the bunch number (0-35) divided by two versus the remainder of Flying Wire Data Freshness variable divided by two.

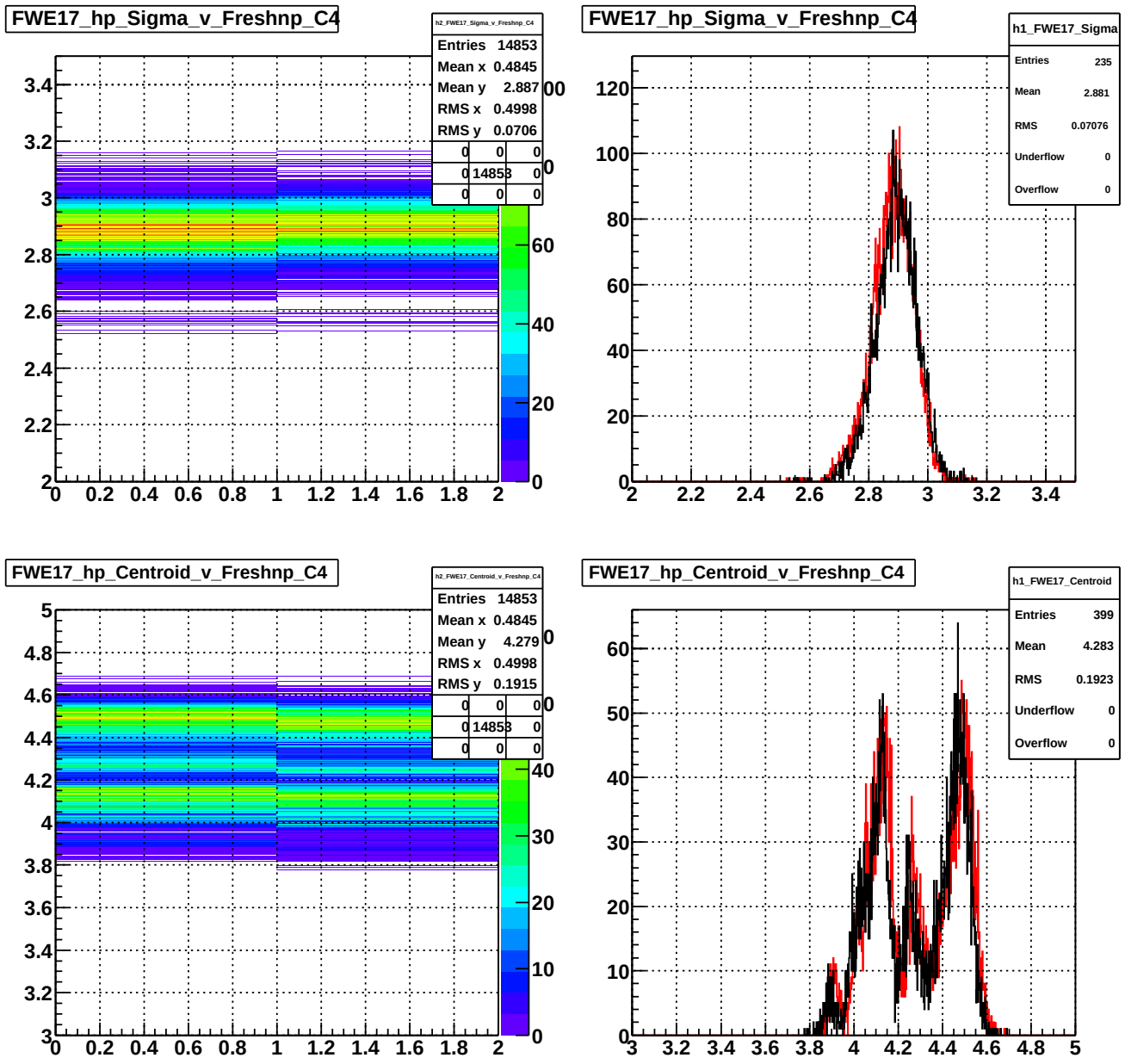

Figure 7: Proton beam, horizontal detector: Performance of the Flying Wire Detector at the E17 location during Tevatron Inject Proton case: sigma of the bunch width distribution (in *mm*) of the FW detector (based on the T:FW[E,H,V][A,P]SE ACNET variable) versus the remainder of Flying Wire Data Freshness variable divided by two (based on the T:FWFRSH ACNET variable); sigma of the bunch width distribution (in *mm*) for odd values of Data Freshness in black and for even values of Data Freshness in red; bunch centroid (in *mm*) position (based on the T:FW[E,H,V][A,P]CE ACNET variable) versus versus the remainder of Flying Wire Data Freshness variable divided by two; bunch centroid (in *mm*) position for odd values of Data Freshness in black and for even values of Data Freshness in red.

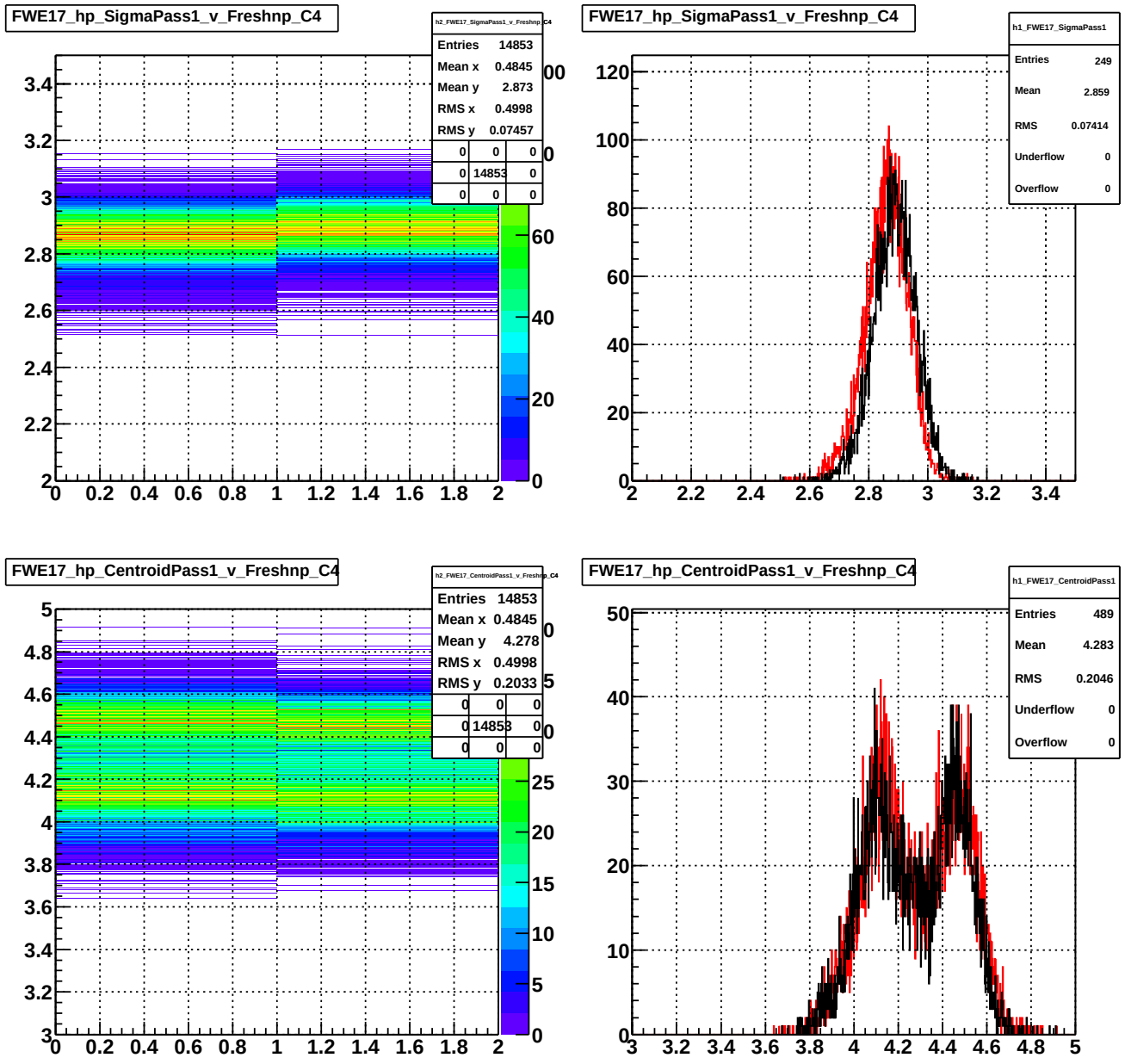

Figure 8: Proton beam, horizontal detector: Performance of the Flying Wire Detector at the E17 location during Tevatron Inject Proton case: pass one sigma of the bunch width distribution (in *mm*) of the FW detector (based on the T:FW[E,H,V][A,P]SE ACNET variable) versus the remainder of Flying Wire Data Freshness variable divided by two (based on the T:FWFRSH ACNET variable); pass one sigma of the bunch width distribution (in *mm*) for odd values of Data Freshness in black and for even values of Data Freshness in red; bunch pass one centroid (in *mm*) position (based on the T:FW[E,H,V][A,P]CE ACNET variable) versus versus the remainder of Flying Wire Data Freshness variable divided by two; bunch pass one centroid (in *mm*) position for odd values of Data Freshness in black and for even values of Data Freshness in red.

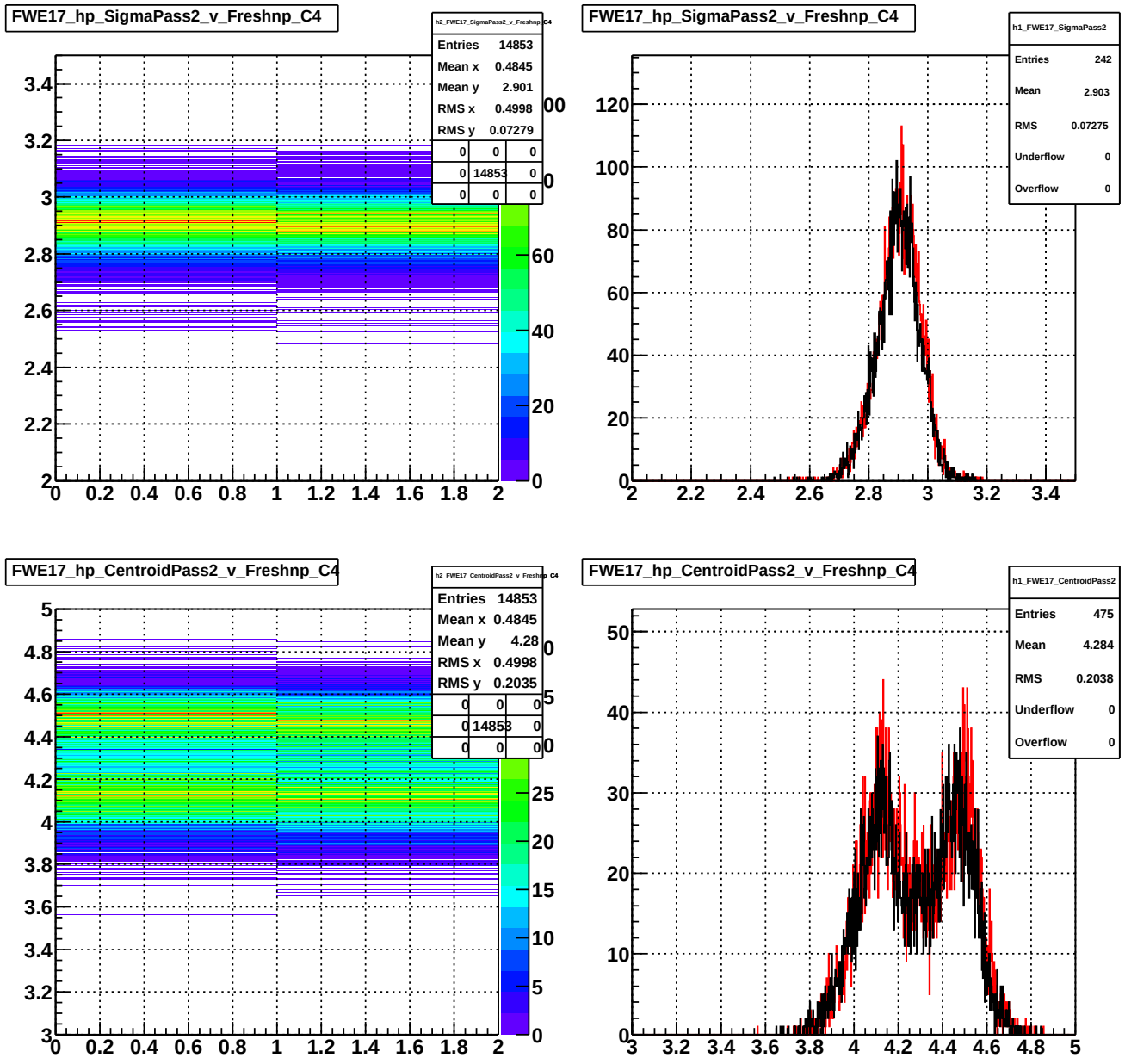

Figure 9: Proton beam, horizontal detector: Performance of the Flying Wire Detector at the E17 location during Tevatron Inject Proton case: pass two sigma of the bunch width distribution (in *mm*) of the FW detector (based on the T:FW[E,H,V][A,P]SE ACNET variable) versus the remainder of Flying Wire Data Freshness variable divided by two (based on the T:FWFRSH ACNET variable); pass two sigma of the bunch width distribution (in *mm*) for odd values of Data Freshness in black and for even values of Data Freshness in red; bunch pass two centroid (in *mm*) position (based on the T:FW[E,H,V][A,P]CE ACNET variable) versus versus the remainder of Flying Wire Data Freshness variable divided by two; bunch pass two centroid (in *mm*) position for odd values of Data Freshness in black and for even values of Data Freshness in red.

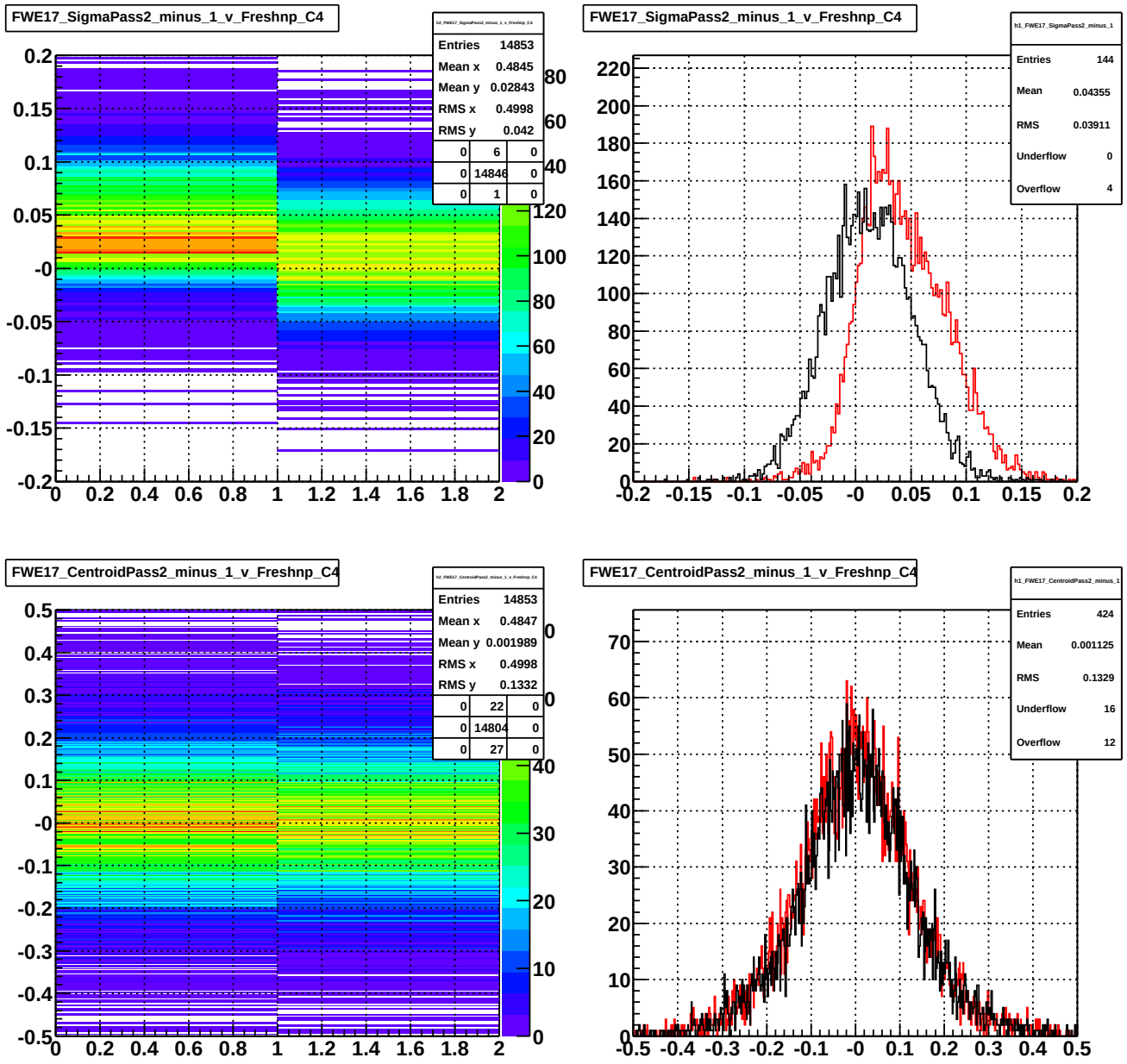

Figure 10: Proton beam, horizontal detector: Performance of the Flying Wire Detector at the E17 location during Tevatron Inject Proton case: sigma pass one minus pass two of the bunch width distribution (in *mm*) of the FW detector (based on the T:FW[E,H,V][A,P]SE ACNET variable) versus the remainder of Flying Wire Data Freshness variable divided by two (based on the T:FWFRSH ACNET variable); sigma pass one minus pass two of the bunch width distribution (in *mm*) for odd values of Data Freshness in black and for even values of Data Freshness in red; bunch centroid pass one minus pass two (in *mm*) position (based on the T:FW[E,H,V][A,P]CE ACNET variable) versus versus the remainder of Flying Wire Data Freshness variable divided by two; bunch centroid pass one minus pass two (in *mm*) position for odd values of Data Freshness in black and for even values of Data Freshness in red.

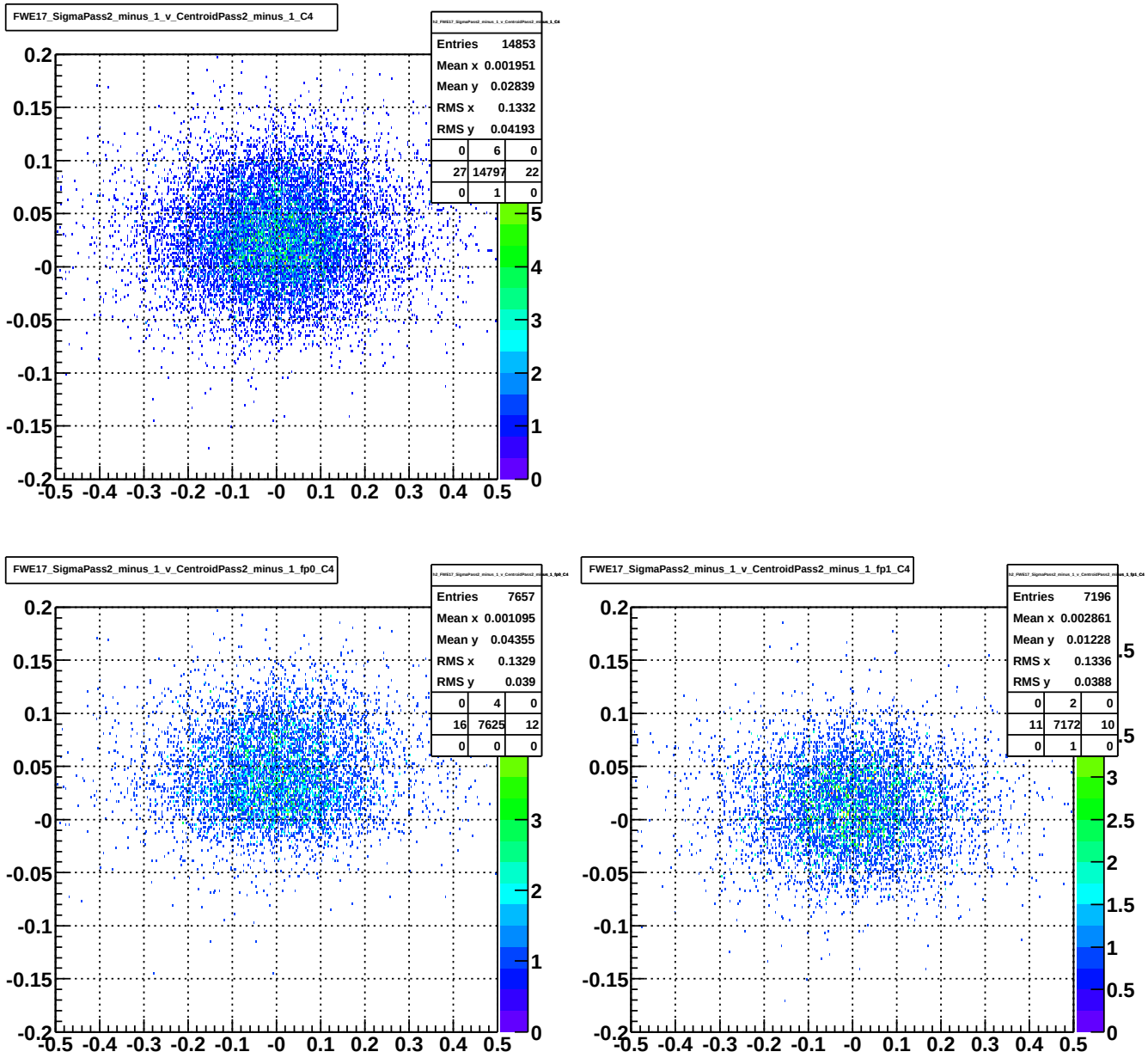

Figure 11: Proton beam, horizontal detector: Performance of the Flying Wire Detector at the E17 location during Tevatron Inject Proton case: sigma pass one minus pass two of the bunch width distribution (in *mm*) of the FW detector (based on the T:FW[E,H,V][A,P]SE ACNET variable) versus bunch centroid pass one minus pass two (in *mm*) position (based on the T:FW[E,H,V][A,P]CE ACNET variable); sigma pass one minus pass two of the bunch width distribution (in *mm*) of the FW detector (based on the T:FW[E,H,V][A,P]SE ACNET variable) versus bunch centroid pass one minus pass two (in *mm*) position (based on the T:FW[E,H,V][A,P]CE ACNET variable) for even values of Flying Wire Data Freshness (based on the T:FWFRSH ACNET variable); sigma pass one minus pass two of the bunch width distribution (in *mm*) of the FW detector (based on the T:FW[E,H,V][A,P]SE ACNET variable) versus bunch centroid pass one minus pass two (in *mm*) position (based on the T:FW[E,H,V][A,P]CE ACNET variable) for odd values of Flying Wire Data Freshness (based on the T:FWFRSH ACNET variable).

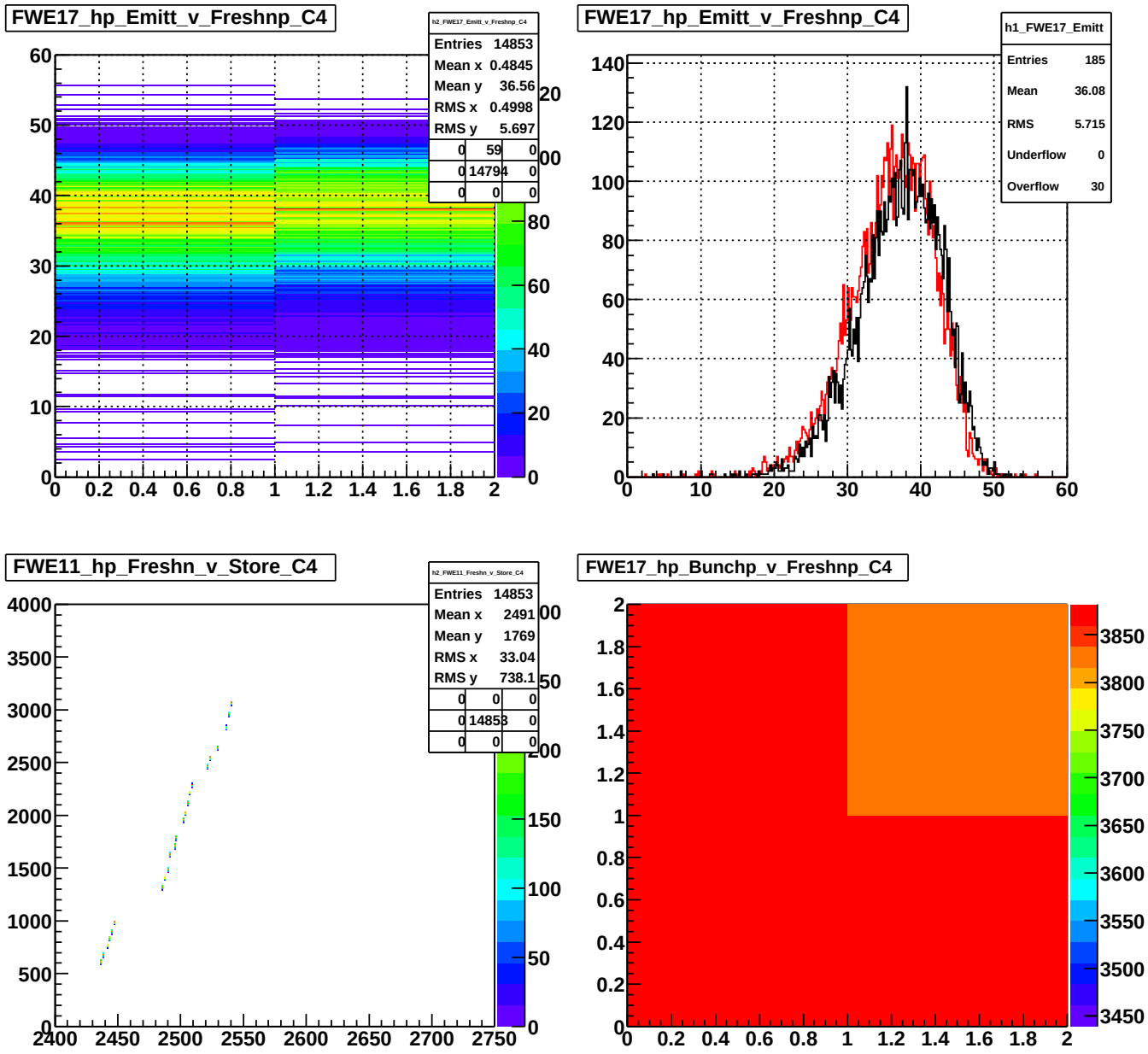

Figure 12: Proton beam, horizontal detector: Performance of the Flying Wire Detector at the E17 location during Tevatron Inject Proton case: bunch emittance (in $\pi \cdot mm \cdot mrad$) versus the remainder of Flying Wire Data Freshness variable divided by two (based on the T:FWFRSH ACNET variable); bunch emittance (in $\pi \cdot mm \cdot mrad$) for odd values of Data Freshness in black and for even values of Data Freshness in red; Data Freshness versus store number; the remainder of the bunch number (0-35) divided by two versus the remainder of Flying Wire Data Freshness variable divided by two.

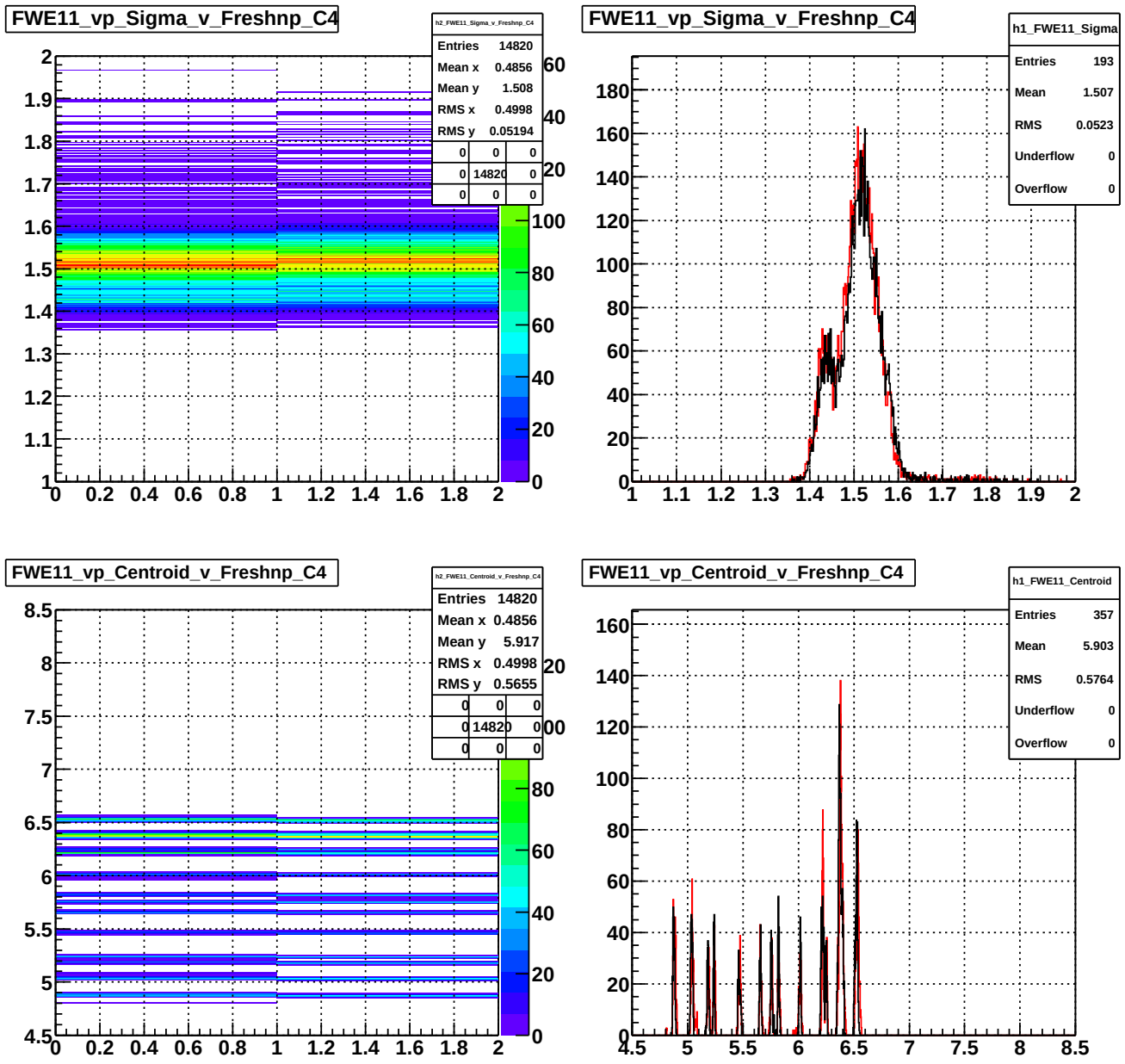

Figure 13: Proton beam, vertical detector: Performance of the Flying Wire Detector at the E11 location during Tevatron Inject Proton case: sigma of the bunch width distribution (in *mm*) of the FW detector (based on the T:FW[E,H,V][A,P]SE ACNET variable) versus the remainder of Flying Wire Data Freshness variable divided by two (based on the T:FWFRSH ACNET variable); sigma of the bunch width distribution (in *mm*) for odd values of Data Freshness in black and for even values of Data Freshness in red; bunch centroid (in *mm*) position (based on the T:FW[E,H,V][A,P]CE ACNET variable) versus versus the remainder of Flying Wire Data Freshness variable divided by two; bunch centroid (in *mm*) position for odd values of Data Freshness in black and for even values of Data Freshness in red.

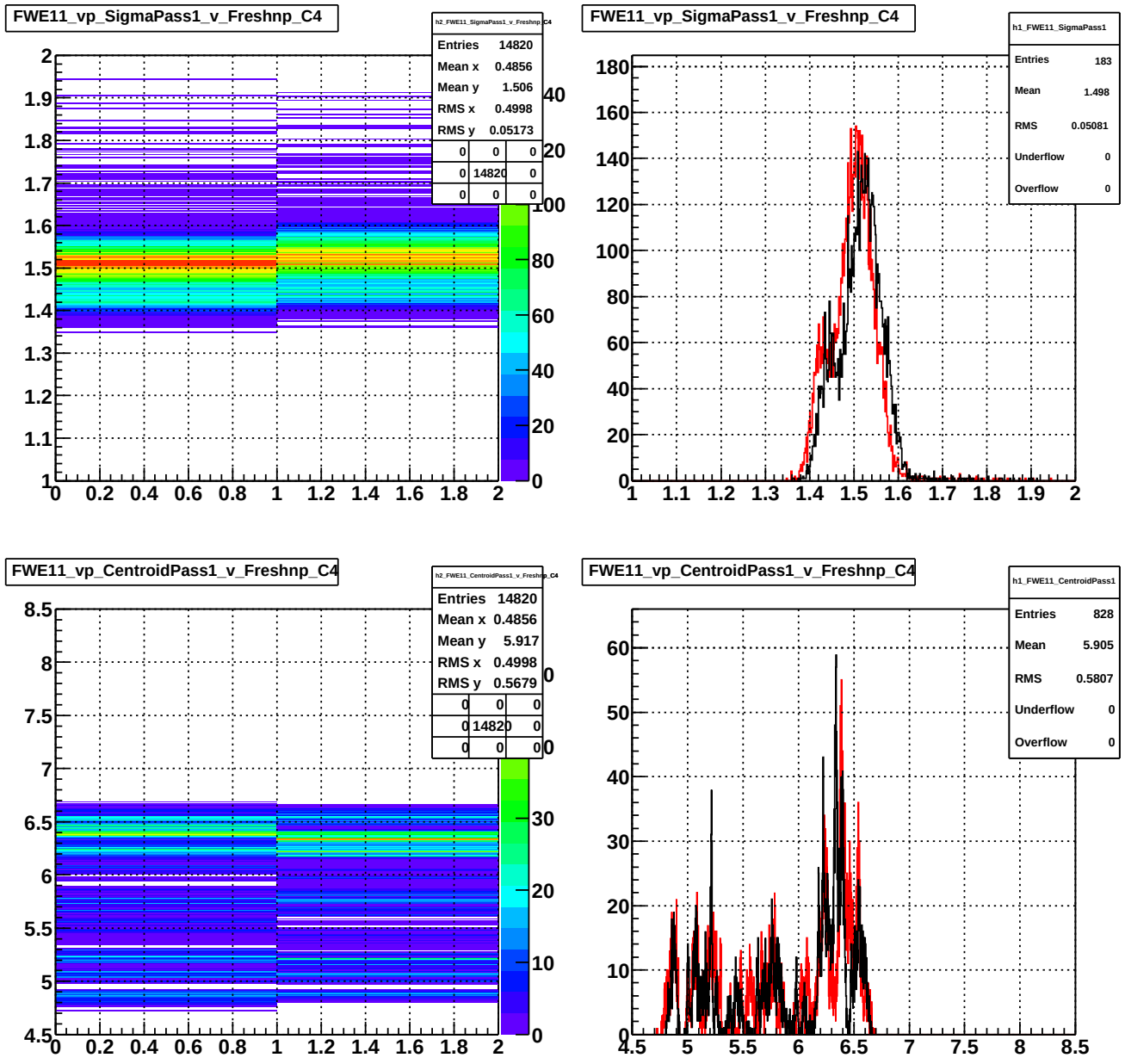

Figure 14: Proton beam, vertical detector: Performance of the Flying Wire Detector at the E11 location during Tevatron Inject Proton case: pass one sigma of the bunch width distribution (in *mm*) of the FW detector (based on the T:FW[E,H,V][A,P]SE ACNET variable) versus the remainder of Flying Wire Data Freshness variable divided by two (based on the T:FWFRSH ACNET variable); pass one sigma of the bunch width distribution (in *mm*) for odd values of Data Freshness in black and for even values of Data Freshness in red; bunch pass one centroid (in *mm*) position (based on the T:FW[E,H,V][A,P]CE ACNET variable) versus versus the remainder of Flying Wire Data Freshness variable divided by two; bunch pass one centroid (in *mm*) position for odd values of Data Freshness in black and for even values of Data Freshness in red.

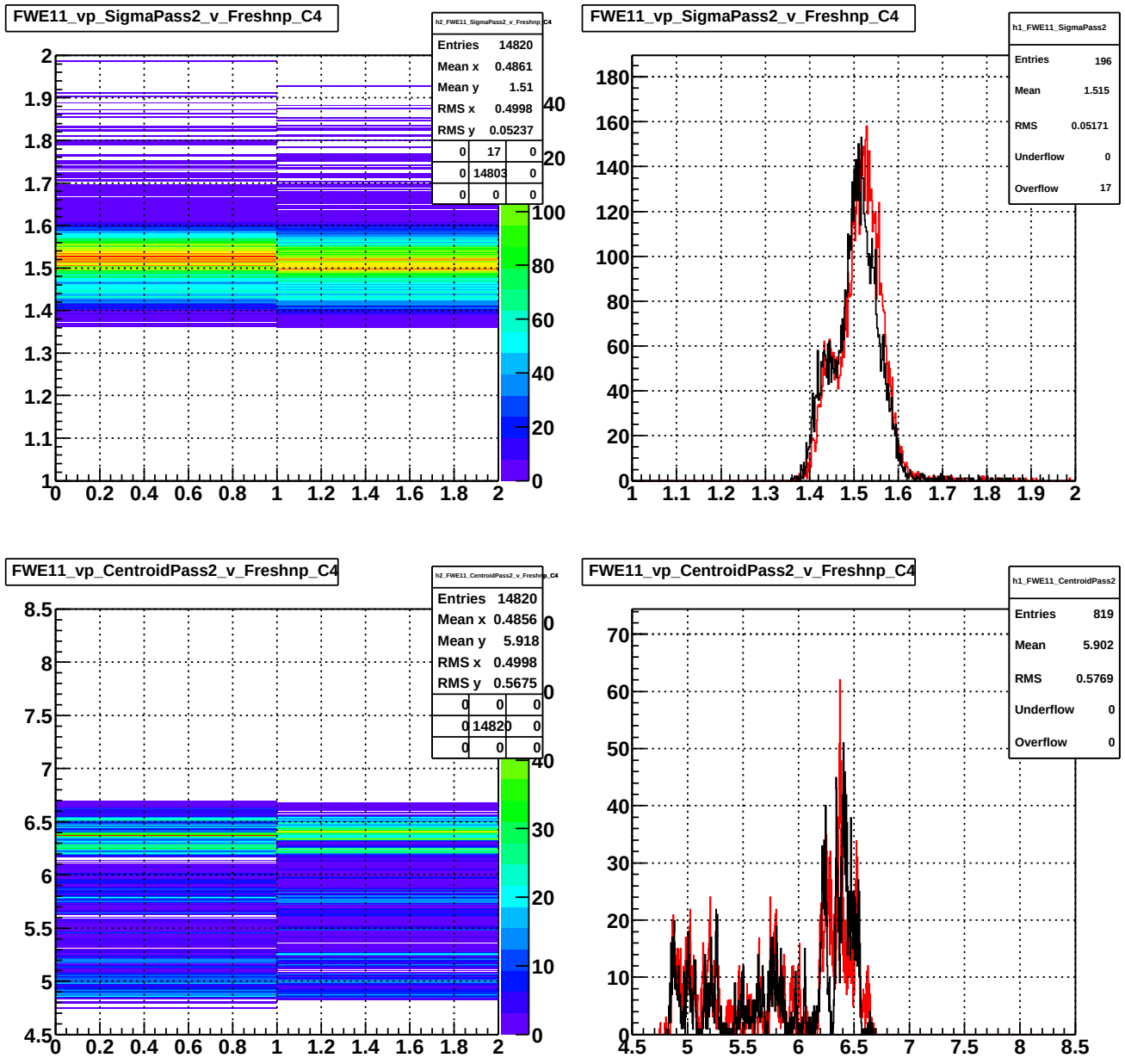

Figure 15: Proton beam, vertical detector: Performance of the Flying Wire Detector at the E11 location during Tevatron Inject Proton case: pass two sigma of the bunch width distribution (in *mm*) of the FW detector (based on the T:FW[E,H,V][A,P]SE ACNET variable) versus the remainder of Flying Wire Data Freshness variable divided by two (based on the T:FWFRSH ACNET variable); pass two sigma of the bunch width distribution (in *mm*) for odd values of Data Freshness in black and for even values of Data Freshness in red; bunch pass two centroid (in *mm*) position (based on the T:FW[E,H,V][A,P]CE ACNET variable) versus versus the remainder of Flying Wire Data Freshness variable divided by two; bunch pass two centroid (in *mm*) position for odd values of Data Freshness in black and for even values of Data Freshness in red.

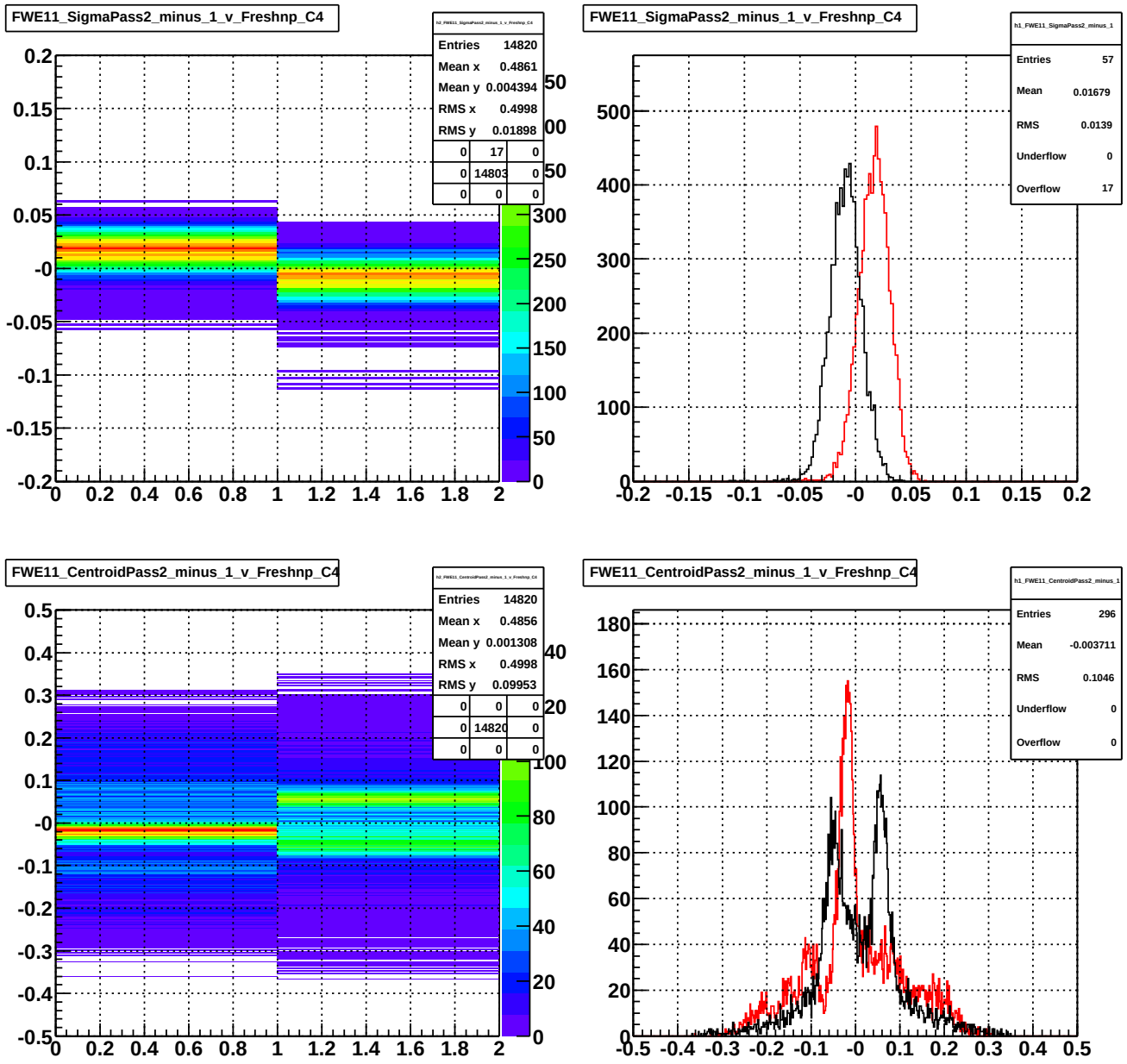

Figure 16: Proton beam, vertical detector: Performance of the Flying Wire Detector at the E11 location during Tevatron Inject Proton case: sigma pass one minus pass two of the bunch width distribution (in *mm*) of the FW detector (based on the T:FW[E,H,V][A,P]SE ACNET variable) versus the remainder of Flying Wire Data Freshness variable divided by two (based on the T:FWFRSH ACNET variable); sigma pass one minus pass two of the bunch width distribution (in *mm*) for odd values of Data Freshness in black and for even values of Data Freshness in red; bunch centroid pass one minus pass two (in *mm*) position (based on the T:FW[E,H,V][A,P]CE ACNET variable) versus versus the remainder of Flying Wire Data Freshness variable divided by two; bunch centroid pass one minus pass two (in *mm*) position for odd values of Data Freshness in black and for even values of Data Freshness in red.

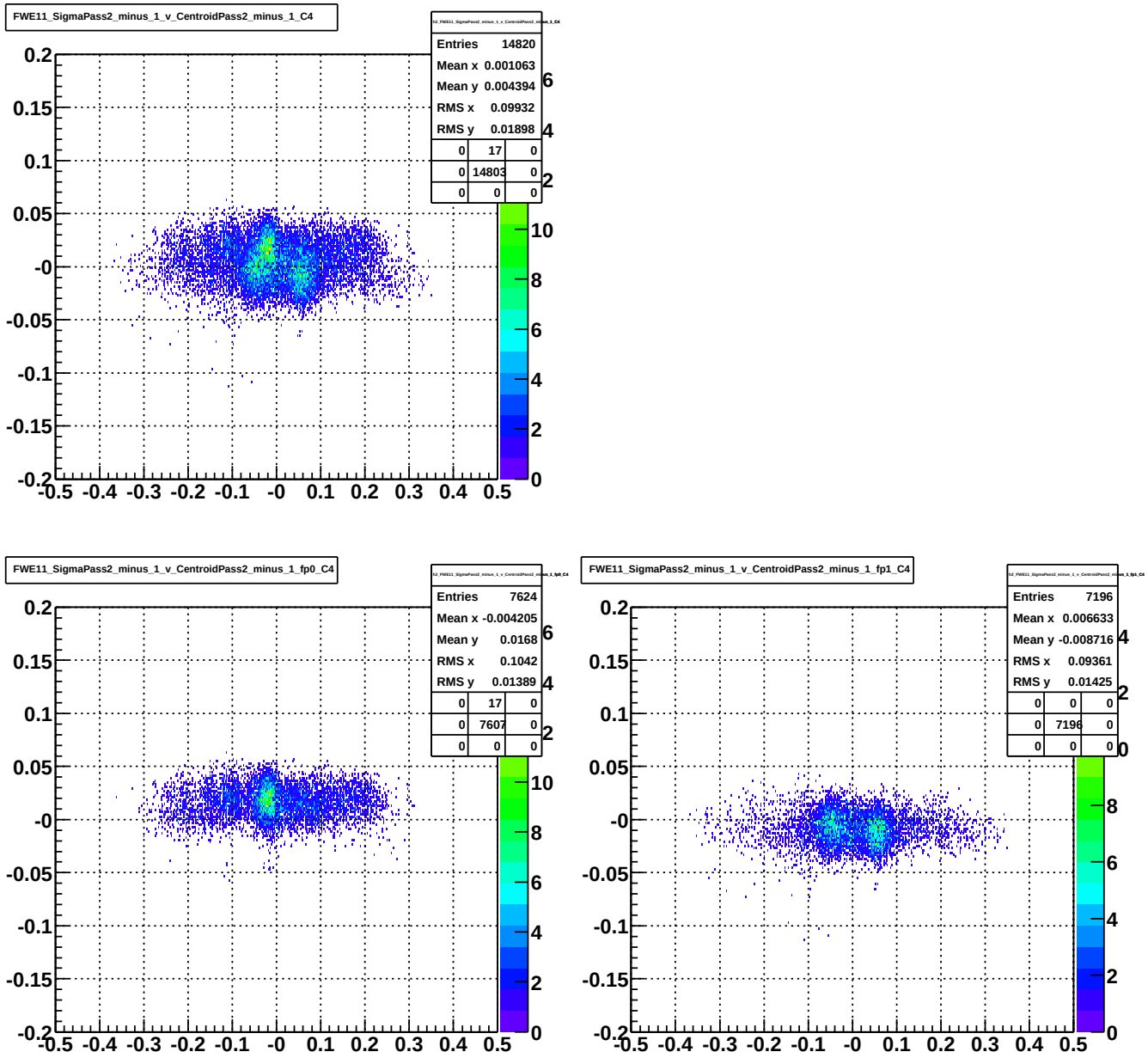

Figure 17: Proton beam, vertical detector: Performance of the Flying Wire Detector at the E11 location during Tevatron Inject Proton case: sigma pass one minus pass two of the bunch width distribution (in *mm*) of the FW detector (based on the T:FW[E,H,V][A,P]SE ACNET variable) versus bunch centroid pass one minus pass two (in *mm*) position (based on the T:FW[E,H,V][A,P]CE ACNET variable); sigma pass one minus pass two of the bunch width distribution (in *mm*) of the FW detector (based on the T:FW[E,H,V][A,P]SE ACNET variable) versus bunch centroid pass one minus pass two (in *mm*) position (based on the T:FW[E,H,V][A,P]CE ACNET variable) for even values of Flying Wire Data Freshness (based on the T:FWFRSH ACNET variable); sigma pass one minus pass two of the bunch width distribution (in *mm*) of the FW detector (based on the T:FW[E,H,V][A,P]SE ACNET variable) versus bunch centroid pass one minus pass two (in *mm*) position (based on the T:FW[E,H,V][A,P]CE ACNET variable) for odd values of Flying Wire Data Freshness (based on the T:FWFRSH ACNET variable).

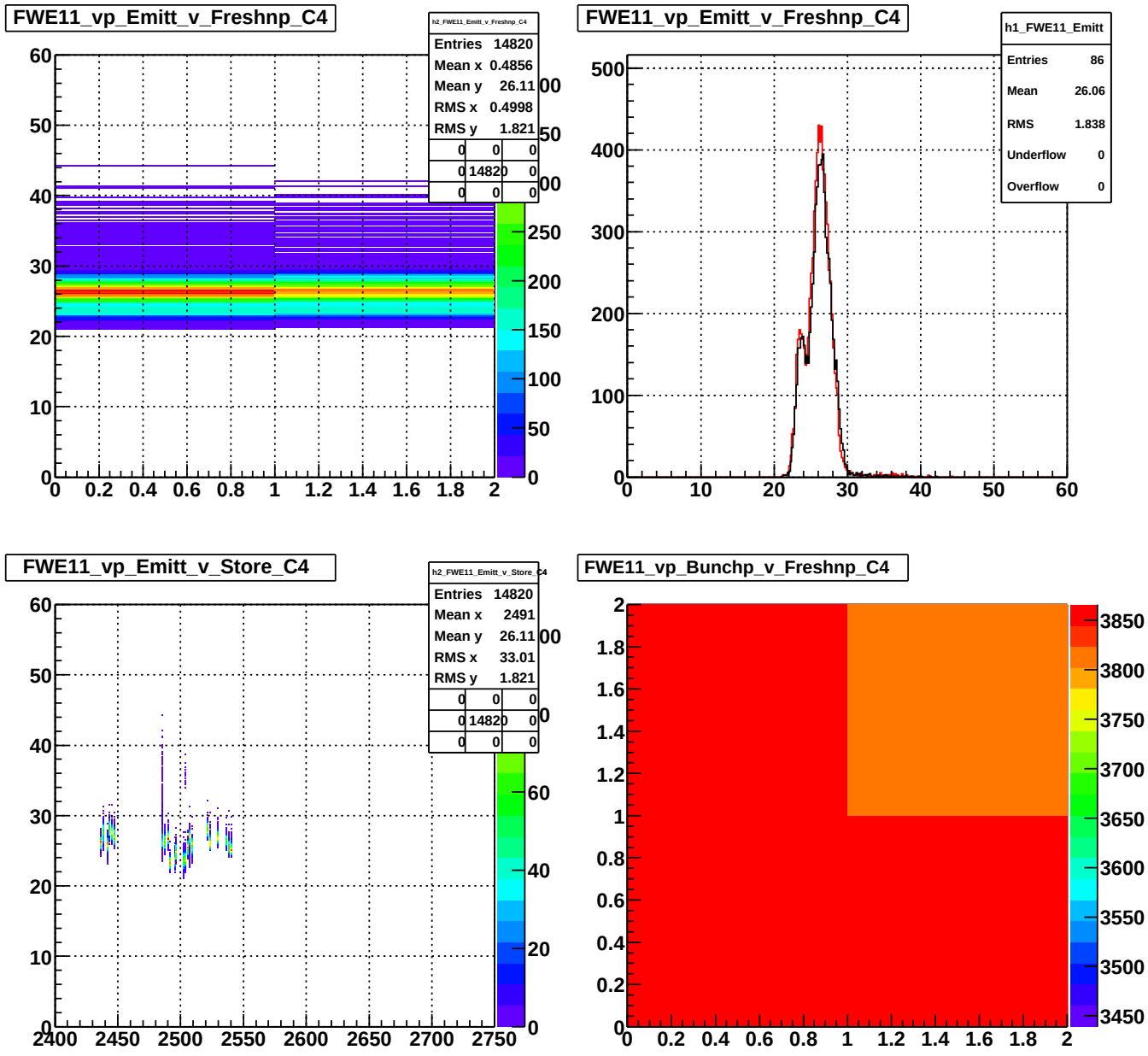

Figure 18: Proton beam, vertical detector: Performance of the Flying Wire Detector at the E11 location during Tevatron Inject Proton case: bunch emittance (in $\pi \cdot mm \cdot mrad$) versus the remainder of Flying Wire Data Freshness variable divided by two (based on the T:FWFRSH ACNET variable); bunch emittance (in $\pi \cdot mm \cdot mrad$) for odd values of Data Freshness in black and for even values of Data Freshness in red; bunch emittance (in $\pi \cdot mm \cdot mrad$) versus store number; the remainder of the bunch number (0-35) divided by two versus the remainder of Flying Wire Data Freshness variable divided by two.